

Accepted Article

Title: Covalently Interlocked Cyclohexa-m-phenylenes and their Assembly: En Route to Supramolecular 3D Carbon Nanostructures

Authors: Bastian Dumslaff, Anna Naima Reuss, Manfred Wagner, Xinliang Feng, Akimitsu Narita, George Fytas, and Klaus Müllen

This manuscript has been accepted after peer review and appears as an Accepted Article online prior to editing, proofing, and formal publication of the final Version of Record (VoR). This work is currently citable by using the Digital Object Identifier (DOI) given below. The VoR will be published online in Early View as soon as possible and may be different to this Accepted Article as a result of editing. Readers should obtain the VoR from the journal website shown below when it is published to ensure accuracy of information. The authors are responsible for the content of this Accepted Article.

To be cited as: *Angew. Chem. Int. Ed.* 10.1002/anie.201705403
Angew. Chem. 10.1002/ange.201705403

Link to VoR: <http://dx.doi.org/10.1002/anie.201705403>
<http://dx.doi.org/10.1002/ange.201705403>

Covalently Interlocked Cyclohexa-*m*-phenylenes and their Assembly:

En Route to Supramolecular 3D Carbon Nanostructures

Bastian Dumschlaff,^[a] Anna N. Reuss,^[a] Manfred Wagner,^[a] Xinliang Feng,^[b] Akimitsu Narita,^[a] George Fytas^[a,c] and Klaus Müllen*^[a]

Abstract: While trying to cluster as many phenylene units as possible in a given space, we proceed to the 3D world of benzene-based molecules by employing covalently interlocked cyclohexa-*m*-phenylenes as present in the unique paddlewheel shaped polyphenylene reported in this work (**10**). A precursor was conceived, in which freely rotating *m*-chlorophenylene units provide sufficient solubility along with the necessary proximity for the final ring closure toward **10**. The assembly of its solubilized *tert*-butyl derivatives to supramolecular carbon nanostructures is subsequently monitored by dynamic light scattering (DLS) and Brillouin light scattering (BLS), revealing the dimension of the initially formed aggregates as well as the amorphous character of the solid state.

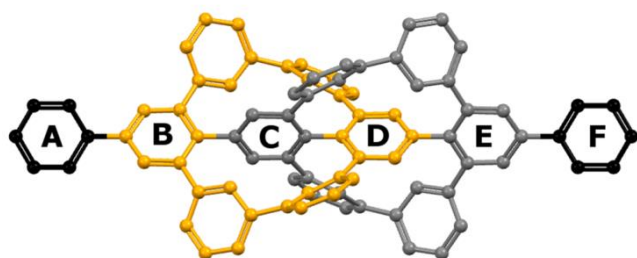


Figure 1. Calculated structure of paddlewheel **10a**.

The benzene ring has proven as a universal modular building block of carbon rich macromolecules^[1] with different sizes, shapes and dimensionalities^[2], ranging from linear (1D) polyphenylenes to disk-type (2D) graphenes and their molecularly defined cutouts^[3]. Considerably less attention has been attracted by 3D carbon nanostructures consisting exclusively of sp²-carbon repeating units^[4]. The tight packing of twisted benzene rings in three-dimensional polyphenylene

macromolecules without significant strain holds promise as a feasible access toward carbon rich materials^[5]. The shape of paddlewheel molecule **10** makes it ideally suited as building block for the construction of bulk 3D carbon nanostructures through a subsequent transition from molecular to supramolecular design^[6]. This assembly process affords carbon rich, solid glasses. The extremely high temperatures of transitions from the solid to the viscous liquid and the small thermal volume expansion point toward a tight and stable packing of molecules. In order to monitor the prevailing hierarchy of structure formation, we perform light scattering experiments on the initial aggregation of **10** in solution toward assemblies comprising at least ten molecules.

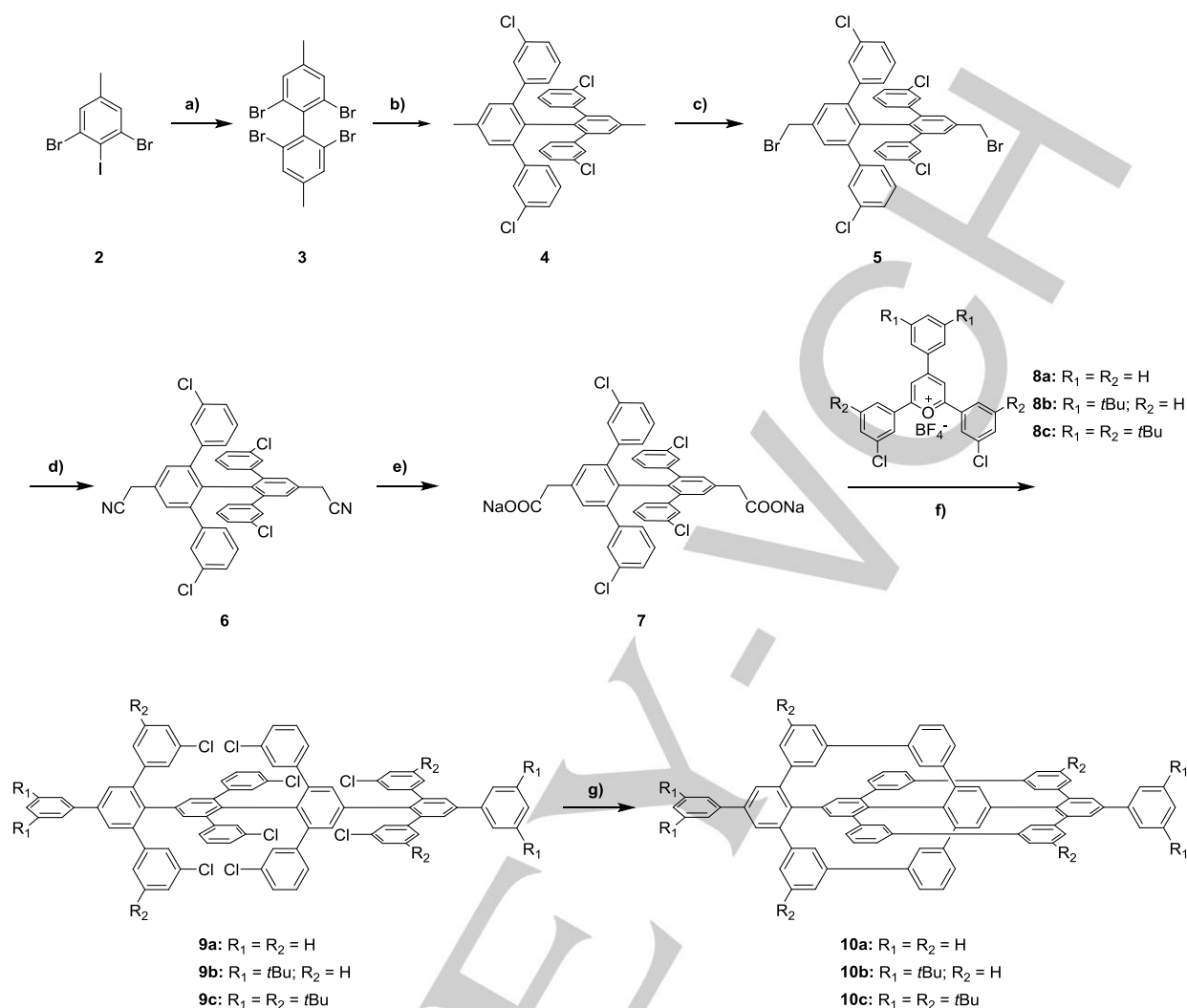
The structural complexity of the title molecule **10** needs some further illustration. As depicted in figure 1, **10a** consists of two orthogonal cyclohexa-*meta*-phenylene units (highlighted in orange and grey), which are covalently interlocked. At the same time, the central phenylene units belonging to the orange cycle (**B** and **D**) and the ones of the grey cycle (**C** and **E**) are part of the rigid sexiphenyl backbone (**A-F**) of **10a**. Two major building blocks are required for the synthesis of **10**: Dicarboxylate **7** as well as the appropriate 2,4,6-triaryl pyrylium salts **8a-c**. Transformation of the pyrylium salts to the respective arenes by condensation with **7** is the key step of the present reaction sequence since exchange of the pyrylium heteroatom by a carbon atom after decarboxylation of **7** provides the precursors **9a-c**. Starting with a functionalized benzene as the simplest aromatic unit, **2** was converted into biphenyl **3** by an oxidative homocoupling. Next, **3** and (*m*-chlorophenyl)boronic acid were subjected to a fourfold Suzuki coupling using our recent protocol^[7] to isolate **4** after recrystallization. The subsequent bromination of the methyl groups of **4** was accomplished by overbromination and subsequent selective debromination to obtain **5**. Introduction of cyano substituents by a modified Kolbe-type cyanation followed by acidic hydrolysis of **6** and the deprotonation of the resulting diphenylacetic acid yielded dicarboxylate **7**. The 2,4,6-triarylpyrylium salts **8a-c** were obtained following a procedure reported by Höger et al.^[8] through a one-pot-reaction using two equivalents of acetophenone and one equivalent of benzaldehyde, respectively, with boron trifluoride diethyl etherate as Lewis acid. The condensation reaction of the two major building blocks **7** and **8a-c** gave the desired octachloro-precursors **9a-c** in moderate yields, which were afterwards converted into the paddlewheel

[a] Bastian Dumschlaff, Anna Reuss, Dr. Manfred Wagner, Dr. Akimitsu Narita, Prof. Dr. George Fytas, Prof. Dr. Klaus Müllen
Max Planck Institute for Polymer Research, Ackermannweg 10, D-55128 Mainz, Germany
E-Mail: muellen@mpip-mainz.mpg.de

[b] Prof. Dr. Xinliang Feng
Center for Advancing Electronics Dresden & Department of Chemistry and Food Chemistry, Technische Universität Dresden, 01062 Dresden, Germany

[c] Prof. Dr. George Fytas
IESL-FO.R.T.H 71110, Heraklion, Greece

Supporting information for this article is given via a link at the end of the document.



Scheme 1. Synthetic route toward **10a-c**. a) *n*-BuLi, CuCl₂, Et₂O, -78 °C→25 °C, 24 h, 55 %; b) (*m*-chlorophenyl)boronic acid, Pd(PPh₃)₄, K₂CO₃, Aliquat 336, toluene, 110 °C, 48 h, 56 %; c) 1. NBS, CCl₄, 80 °C, 24 h; 2. DIPEA, P(OEt)₂(O)H, THF, 0 °C→25 °C, 48 h, 80 %; d) KCN, TBAHS, DCM/water, 25 °C, 48 h, 95 %; e) 1. HBr, AcOH, TBAF, 105 °C, 48 h; 2. NaOMe, MeOH, 24 h, 99 %; f) acetic anhydride, 160 °C, 24 h, 11-31 %; g) [Ni(COD)₂], 2,2'-bipyridine, THF/COD, microwave 300W, 90 °C, 8 h, 97-99 %.

structures **10a-c** through Yamamoto coupling of the pre-organized *m*-chlorophenylene units. A high catalyst load was essential together with microwave irradiation under inert conditions. The title structure was isolated by precipitating the reaction mixture in methanol/hydrochloric acid 1:1 and washing the residue with a mixture of methanol and THF several times to assure that no incompletely closed sideproducts were present, which could be confirmed by MALDI-ToF spectrometry (see figure 2) and NOESY (see figure S20).

Remarkably enough, the colorless solid **10a** features an extremely high thermal stability with no weight loss up to 450 °C by thermal gravimetric analysis TGA (see S45). Comparison of the IR-spectra of **10a** and its precursor **9a** clearly reveals the vanishing C=C stretching (out-of-plane) vibration of the freely rotating phenylene units ($\nu=1600\text{ cm}^{-1}$ ^[9], see S40) and indicates the intramolecular reaction. Due to the terminal phenyl units, a

residual IR-band with low intensity is still observable at the corresponding wave number. The absorption band of the UV/Vis spectrum of **10a** shows a redshift compared to the unclosed octachloro-precursor **9a** (see figure S37, shift from 277 nm to 317 nm), indicative of an increasing conjugation.

The high resolution (HR) MALDI-ToF-MS spectrum of **10a** displays an intense signal with $m/z = 1058.4244$ matching the expected molar mass of **10a** ($m/z = 1058.3913$). The isotopic distribution (inset figure 2, red line) is fully consistent with the simulated spectrum calculated from the elemental composition of C₈₄H₅₀ (inset figure 2, black line). The structure of **10a** was furthermore proven by 1H-1H-nuclear-Overhauser-effect-spectroscopy (NOESY), where the highly resolved signals and the corresponding proton-correlations agree with the claimed paddlewheel structure of **10a** (see S20). These signals are superimposed on a broad background signal which we interpret

by the strong tendency toward aggregation but not by the existence of oligomeric sideproducts. This assumption is consistent with light scattering results (see below) and with evidence from the MALDI-ToF-MS spectrum where a second signal with low intensity can be observed at exactly twice the mass of **10a**. Note that a covalently bonded dimer would appear at two times the mass of **10a** minus two hydrogen atoms, which could never be observed for **10a** and its substituted congeners **10b** and **10c** (see S34). The rigid shape and the aggregation properties of **10a** are important for the packing toward solid 3D carbon nanostructures in bulk and thus the transition from molecular to supramolecular design, but hamper an investigation of its solution behavior. Therefore, four and eight, respectively, bulky *tert*-butyl groups were introduced into the parent compound **10a** by employing the pyrylium salts **8b** and **8c** to provide the substituted structures **10b** and **10c**.

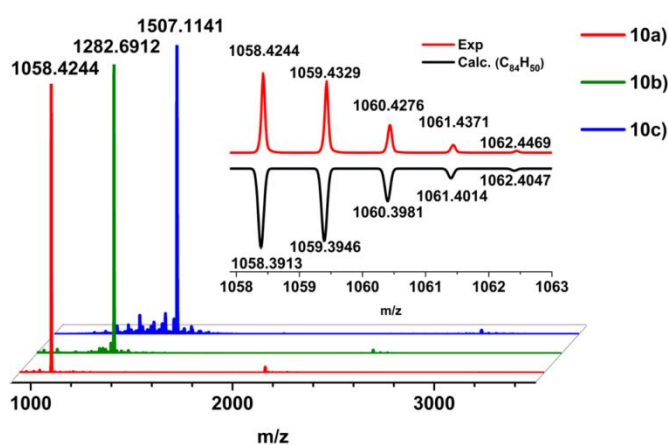


Figure 2. HR-MALDI-ToF-MS spectra. The main plots show the high resolution MALDI-ToF-MS spectra of **10a** (red); **10b** (green); **10c** (blue), respectively. The inset displays the isotopic distribution of **10a**; the small side peaks in the spectra of **10b** and **10c** are caused by the loss of *tert*-butyl groups due to the high laser power that is necessary to ionize the large molecules.

It appears from the single-crystal structures of **9b** and **9c** (see S53) that the sexiphenyl backbone of **9b** is tilted by 7°, destroying the C_2 symmetry, whereas **9c** shows a perfect C_2 symmetry (see figure 3).

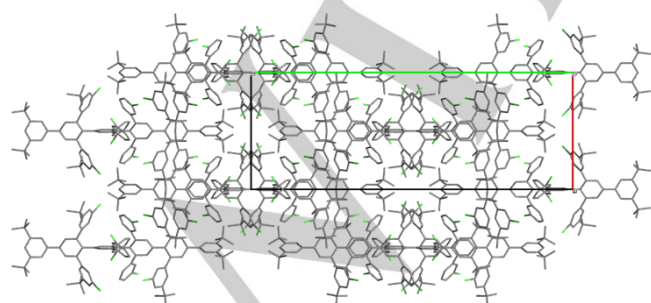


Figure 3. Single crystal structure of **9c**. Packing along *c*; for a better overview hydrogen atoms and solvent molecules are hidden.

The increased solubility of **10b** and **10c** allowed us to monitor the initial stage of supramolecular structure formation by DLS. It probes the translational diffusion of the moieties over a selected length $2\pi/q$ through the relaxation function $C(q,t)$ (figure 4a). Quite characteristically, the observed time decay cannot be represented by a single exponential function at both concentrations used. Instead, two populations are needed as shown by the inverse-Laplace transformation of $C(q,t)$ (species 1 and 2) in figure 4a. Based on the scattering intensity and the diffusion coefficient, species 1 has a hydrodynamic radius of $R_h = 3.7$ nm. Using this value, the size of the formed supramolecular nanostructure can be calculated. It comprises about ten molecules of **10b** which are assumed to assemble side-by-side with their long axes parallel to each other (see figure 4c).

The structural motif of **10** shows large cavities at its periphery due to the orthogonally arranged cyclohexa-*meta*-phenylene units causing the formation of lateral aggregates (see figure 4c).

The about 10-times slower diffusion of species 2 corresponds to much larger and also concentration-dependent aggregates of **10b**. The solution of **10c** displays a much weaker light scattering intensity, and $C(q,t)$ (see S48) is much faster than for **10b**. The experimental diffusion coefficient suggests either a cylinder (eq. S6-S8) with a length of $l = 3$ nm and a diameter of $d = 1.1$ nm or an ellipsoid of revolution (eq. S3-S5) with a 1.5 nm and 0.7 nm long and short semi-axes, respectively. Both models yield the size of a single **10c** molecule (calculated $l = 2.8$ nm, $d = 1.2$ nm). It can thus be concluded that the additional four *tert*-butyl groups in the periphery largely suppress the side-by-side stacking as observed in **10b**.

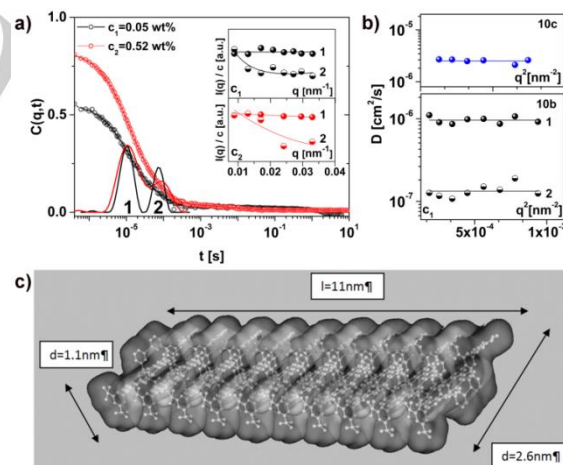


Figure 4. Aggregation behavior of **10b** in dilute solutions. a: Relaxation function $C(q,t)$ recorded by dynamic light scattering at a scattering wave vector q for **10b** in chloroform at two concentrations. The translational motion over a length of about 190 nm ($\sim 2\pi/q$) reveals two distinct populations of species 1 and 2 with different sizes as indicated by the distinct q -dependence of the associated intensities (top and bottom inset); b: two diffusion coefficients in the lowest concentration of **10b** (bottom inset to figure 4b). The diffusion coefficient of **10c** in chloroform (0.2 wt%) (top inset to figure 4b); c: suggested model for a lateral aggregate of **10b** consisting of ten molecules

Having proven the importance of solubility tuning and the strong propensity of **10b** toward aggregate formation, one could now

consider the solid state properties of the resulting 3D carbon nanostructures. The two precursors **9b** and **9c** are crystalline whereas the paddlewheel structures **10b** and **10c** are amorphous solids (glasses) at ambient conditions. Given their relatively high density (see tables S3 and S4), the transition to the fluid state is anticipated to occur at high temperatures compared to known molecular glass formers^[10]. We employed the non-destructive and non-contact Brillouin light scattering technique (BLS) to probe the solid state of **10b** and **10c** as a function of temperature. The temperature dependence of the longitudinal sound velocity in **10b** and **10c** is shown in the main plot of figure 5a along with the BLS spectra of **10b** of the longitudinal phonons (VV) in the top part of figure 5b.

In contrast to **10b**, the analogue **10c** undergoes a transition from glass to viscous liquid at $T_g \sim 152$ °C (shaded area) as indicated by the change of the slope in Figure 5a. Such high T_g values for molecular glass formers have, to the best of our knowledge, never been reported. We rationalize the unexpectedly high T_g and the larger span of the glassy state for **10b** by considering the thermal volume expansion since it is related to phase transitions: The state of a material depends on the maximum amount of potentially compressible (thus “free”) space available in a closest packing^[11] and it is therefore not the total volume (V), but the free volume (V_f) that controls the evolution of a state with temperature. The sound velocity data from Figure 5 can be used to estimate the relative thermal volume expansion in **10b** and **10c**. The slope is proportional to the thermal expansion coefficient of the material, but only for **10c** is the slope accessible and hence the fractional free volume V_f/V above T_g . Due to the experimentally inaccessible T_g of **10b**, its dimension has to be extrapolated by adding the well-known molecular glass former trinaphthylbenzene (TNB) for comparison, for which BLS data have been reported^[11] (figure S50). With $T_g = 60$ °C, TNB has a much lower transition from glass to a viscous liquid than **10c**. The behavior of **10b** must be extrapolated as it possesses a higher density than **10c** (due to the peripheral *tert*-butyl groups). Thus, the high T_g of **10c** and the even higher approximated T_g of **10b** can be attributed to their small thermal volume expansion caused by its tight, stable packing which is only lost at very high temperatures. A tight packing of benzene rings is thus established not only in polyphenylene **10**, but also in its solid supramolecular 3D carbon nanostructures.

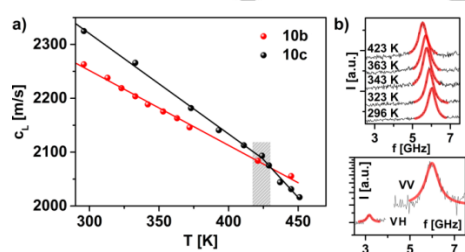


Figure 5. Phase state of **10b** and **10c** by Brillouin light scattering. a: The variation of the longitudinal sound velocity in **10b** (red) and **10c** (black) with temperature. The shaded area indicates the glass transition region of **10c**. b: the polarized spectra for **10b** (top part). Low part: Polarized (VV) and depolarized (VH) spectra of **10b** at 295 K recorded at a wave vector $q = 0.017$ nm⁻¹ corresponding to a phonon wavelength $\Lambda (= 2\pi/q) \sim 370$ nm.

We have introduced complex, but essentially strain-free and thermally stable paddlewheel polyphenylenes **10**. The unprecedented title molecules arise from cyclization of pre-arranged precursors and consist exclusively of benzene rings connected in a “catenane related” motif of two covalently bound, orthogonal cyclohexa-*meta*-phenylene units. Molecular structure proof, while reliably obtained from spectroscopic data, was hampered by the low solubility of the rigid, carbon rich molecule **10a**. This suggested to turn vice into virtue and to employ it as building block of supramolecular aggregate formation en route to a novel type of bulk 3D carbon nanostructure. The assembly of **10** to increasingly larger aggregates was studied by dynamic light scattering for the solubilized analogues **10b** and **10c**. DLS also furnishes a model for the structure of an initially formed non-covalently bound aggregate comprising at least ten molecules. Different from their crystalline precursors **9b** and **9c**, the corresponding paddlewheel structures **10b** and **10c** exist as amorphous (glassy) materials. While **10c** shows a transition from glass to fluid within the measured temperature range, **10b** is assumed to have a much higher T_g caused by a smaller thermal volume expansion due to its tighter packing. Nevertheless, both molecules possess a much lower thermal volume expansion than comparable aromatic structures, e.g. triarylbenzenes such as TNB. This points toward a very tight, stable packing in the resulting three-dimensional nanostructured motifs. The synthesis of a complex polyphenylene such as **10** and its subsequent assembly to a bulk material are an exemplary case of hierarchical structure formation. This work thus opens a new access to the world of 3D carbon materials by a combination of molecular and supramolecular design and will also stimulate the search for more carbon allotropes.

Acknowledgements

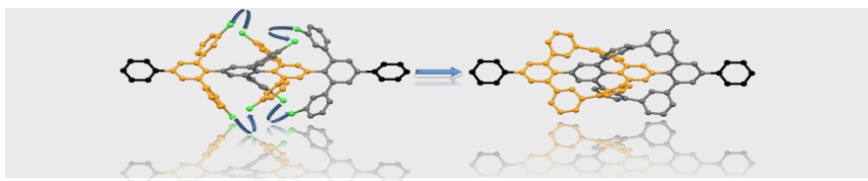
This work was financially supported by European Research Council grant on NANOGRAPH, DFG Priority Program Graphene SPP 1459, the Max Planck Society, and the European Commission through Graphene Flagship. We thank S. Türk and J. Schnee for high-resolution MALDI-ToF-MS analysis, A. Larsen (IESL-FO.R.T.H, Heraklion, Greece) for the dynamic light scattering experiments and D. Schollmeyer for the x-ray diffraction analysis.

Keywords: macrocycles, nanostructures, polyphenylenes, supramolecular chemistry, synthesis design

- [1] A. J. Berresheim, M. Müller, K. Müllen, *Chem. Rev.* **1999**, *99*, 1747-1786.
- [2] a) D. Mössinger, D. Chaudhuri, T. Kudernac, S. Lei, S. De Feyter, J. M. Lupton, S. Höger, *J. Am. Chem. Soc.* **2010**, *132*, 1410-1423; b) C. D. Simpson, J. D. Brand, A. J. Berresheim, L. Przybilla, H. J. Räder, K. Müllen, *Chem. Eur. J.* **2002**, *8*, 1424-1429; c) X. Zhuang, Y. Mai, D. Wu, F. Zhang, X. Feng, *Adv. Mat.* **2015**, *27*, 403-427.
- [3] a) A. K. Geim, K. S. Novoselov, *Nat. Mater.* **2007**, *6*, 183-191; b) J. C. Meyer, A. K. Geim, M. I. Katsnelson, K. S. Novoselov, T. J. Booth, S. Roth, *Nature* **2007**, *446*, 60-63; c) C. D. Simpson, G. Mattersteig, K. Martin, L. Gherghel, R. E. Bauer, H. J. Räder, K. Müllen, *J. Am. Chem. Soc.* **2004**, *126*, 3139-3147.

- [4] X. Shen, D. M. Ho, R. A. Pascal, *J. Am. Chem. Soc.* **2004**, *126*, 5798-5805.
- [5] a) J. Gibson, M. Holohan, H. L. Riley, *J. Chem. Soc. (Resumed)* **1946**, 456-461; b) X. Shen, D. M. Ho, R. A. Pascal, *Org. Lett.* **2003**, *5*, 369-371; c) D. Türp, T.-T.-T. Nguyen, M. Baumgarten, K. Müllen, *New J. Chem.* **2012**, *36*, 282-298.
- [6] J.-M. Lehn, *C. R. Chim.* **2011**, *14*, 348-361.
- [7] F. Schlütter, T. Nishiuchi, V. Enkelmann, K. Müllen, *Polym. Chem.* **2013**, *4*, 2963-2967.
- [8] a) C. Mahler, U. Muller, W. M. Muller, V. Enkelmann, C. Moon, G. Brunklaus, H. Zimmermann, S. Hoger, *Chem. Commun.* **2008**, 4816-4818; b) G. Ohlendorf, C. W. Mahler, S.-S. Jester, G. Schnakenburg, S. Grimme, S. Höger, *Angew. Chem. Int. Ed.* **2013**, *52*, 12086-12090.
- [9] G. Socrates, *Infrared and Raman Characteristic Group Frequencies: Tables and Charts*, 3rd ed., Wiley, **2004**.
- [10] a) K. L. Kearns, T. Still, G. Fytas, M. D. Ediger, *Adv. Mat.* **2010**, *22*, 39-42; b) E. Núñez, C. G. Clark, W. Cheng, A. Best, G. Floudas, A. N. Semenov, G. Fytas, K. Müllen, *J. Phys. Chem. B* **2008**, *112*, 6542-6549.
- [11] R. P. White, J. E. G. Lipson, *Macromolecules* **2016**, *49*, 3987-4007.

COMMUNICATION



Essentially strain-free and thermally stable paddlewheel polyphenylenes consisting of two covalently interlocked cyclohexa-*m*-phenylenes were synthesized. Solubility tuning allowed us to monitor the hierarchical structure formation of 3D carbon nanostructures.

*B. Dumslaff, A. N. Reuss, M. Wagner, X. Feng, A. Narita, G. Fytas and K. Müllen**

Page No. – Page No.

Covalently Interlocked Cyclohexa-*m*-phenylenes and Their Assembly:

En Route to Supramolecular 3D Carbon Nanostructures